DOI: 10.61782/fa.2025.0196

FORUM ACUSTICUM EURONOISE 2025

Characterization of the adhesion quality in an aeronautical assembly by acoustic microscopy

Youness Ezziani[1], Damien Leduc[1], Pierre Maréchal[1], Mounsif Ech-Cherif El-Kettani[1*]
Mathieu Ducousso[2], Nicolas Cuvillier[2]
[1] LOMC, UMR 6294 CNRS, University of Le Havre Normandy, 75 Rue de Bellot, 76600 Le Havre, France.
[2] Safran Tech, Rue des Jeunes Bois, Chateaufort, 78772 Magny-les-Hameaux, France.

ABSTRACT

This work deals with the characterization of the adhesion quality and of the adhesive film properties in Titanium/Epoxy adhesive film/3D Composite aeronautical assemblies. Due to the thickness of the adhesive film in the different samples, between 80 µm and 200 µm, the study is carried out with a scanning acoustic microscope (SAM) in pulse-echo mode, at high frequencies (20 and 50 MHz). The difficulties expected and that are challenged are due both to the acoustic impedance contrast between the materials and to the high frequency of the study, which should render the reflected echo at the Epoxy film/Composite undetectable or very low. These conditions mean that the experiment must be carried out carefully and with high accuracy.
Nevertheless, the observation of the low amplitude reflected echo at the adhesive film/Composite interface in the different samples was possible thanks to the good signal-to-noise ratio (SNR) of the experimental set up instrumentation. The properties of the adhesive film are determined using the A-scan method with a planar transducer. Moreover, SAM images are obtained using a focused transducer, confirming the adhesion quantification and providing a fast estimation of the adhesive film thickness.

Keywords: *ultrasound characterization, scanning acoustic microscope (SAM), composite material, adhesive, high frequency transducer.*

[*] ***Corresponding author***: *echcherm@univ-lehavre.fr*

1. INTRODUCTION

Reducing the weight of aeronautical structures is essential to reduce fuel consumption and emissions. Adhesive bonding, which offers several advantages over traditional methods such as welding or riveting, plays a key role in achieving this weight reduction. Consequently, non-destructive evaluation (NDE) [1, 2] is required to assess the quality of the adhesion in the assemblies. Various NDE techniques are used to detect defects such as porosity or delamination [3]. This study focuses on samples representative of the Leap engine fan blade, provided by Safran Tech, which consists of a titanium alloy TA6V {Ti} bonded to a thick 3D woven Composite {Comp} with a thin layer of Epoxy resin AF191K {Epo} in the range of a hundred microns. The resulting structure is a trilayer stack {Ti/Epo/Comp}. Its properties are given on Table 1. Due to the thickness and properties of the Composite, it is considered as a semi-infinite medium in the frequency range of the study. To achieve effective echo separation, the axial resolution of the selected transducer must be appropriately matched to the adhesive layer thickness, typically ensured by maintaining a sufficient thickness-to-wavelength ratio. As a result, thin adhesive layers require a transducer with a center frequency in the tens of MHz range. Until now, obtaining reliable information on adhesion levels has been challenging, as it is highly dependent on the adhesive thickness and on the acoustic impedance ratios. The difficulty in performing ultrasonic evaluations with a favorable signal-to-noise ratio stems from the significant acoustic impedance contrast between TA6V and the Epoxy resin, and the relatively low contrast between the Epoxy resin and the Composite. This contrast, together with the attenuation introduced by the high frequency of the study, make the detection of the reflected echo at the Epoxy/Composite interface particularly

challenging. It is therefore crucial to find a balance: a frequency high enough to match the wavelength to the adhesive's thickness, but not too high (as the attenuation increases with the frequency) to detect background echoes, particularly the background echo at the Adhesive/Composite interface, with a sufficiently exploitable amplitude. The theoretical energy reflection and transmission coefficients for each interface in the assembly at normal incidence are as follows:

R_1 and T_1 (eq. (1)) correspond to the {Water/Ti} interface, R_2 and T_2 (eq. (2)) to the {Ti/Epoxy} interface, and finally R_3 and T_3 (eq. (3)) to the {Epo/Comp} interface.

$$\begin{cases} R_1 = \left(\dfrac{Z_{Ti} - Z_{Water}}{Z_{Ti} + Z_{Water}} \right)^2 \approx 0.8025 \\ T_1 = \dfrac{4 Z_{Ti} Z_{Water}}{\left(Z_{Ti} + Z_{Water} \right)^2} \approx 0.1975 \end{cases} \quad (1)$$

$$\begin{cases} R_2 = \left(\dfrac{Z_{Epo} - Z_{Ti}}{Z_{Epo} + Z_{Ti}} \right)^2 \approx 0.6393 \\ T_2 = \dfrac{4 Z_{Epo} Z_{Ti}}{\left(Z_{Epo} + Z_{Ti} \right)^2} \approx 0.3607 \end{cases} \quad (2)$$

$$\begin{cases} R_3 = \left(\dfrac{Z_{Comp} - Z_{Epo}}{Z_{Comp} + Z_{Epo}} \right)^2 \approx 0.0452 \\ T_3 = \dfrac{4 Z_{Comp} Z_{Epo}}{\left(Z_{Comp} + Z_{Epo} \right)^2} \approx 0.9548 \end{cases} \quad (3)$$

At the {Water/Ti} interface, approximately 80.25% of the energy is reflected, and only 19.75% is transmitted to the Ti layer. At the {Ti/Epo} interface, 63.93% of T_1 is reflected due to the significant impedance contrast between the two materials, while only 4.52% of the product T_1T_2 is reflected at the {Epo/Comp} interface. As a result, very small quantity of energy reaches the {Epo/Comp} interface, and then the reflection at the {Epo/Comp} interface is very weak due to the low impedance contrast between Epoxy and Composite.

2. EXPERIMENT

2.1 Studied samples

The samples studied are representative of the Leap engine fan blade and were provided by Safran Tech. They consist of three materials: a titanium alloy TA6V {Ti} bonded to a thick 3D woven Composite {Comp} using an Epoxy resin AF191K {Epo}. The Epoxy bonding process involves cleaning the interfaces with ethanol. Strips of the chosen material and specific thickness are then placed along the edges of the surfaces between the two materials to control the Epoxy layer thickness and prevent adhesive leakage during polymerization [1]. The polymerization process is carried out in a pressure-controlled oven, where four calibrated spring clamps apply a constant force of 65 N. Under standard conditions, the bonded sample is fully polymerized at 150°C for 3 h [1]. The adhesive thickness was estimated by in a first-hand simply by measuring the entire assembly with a caliper and subtracting the thickness of the titanium alloy and the Composite, as these are relatively thick. The parameters of the samples are given in Table 1, as supplied by the manufacturer.

Table 1. Properties of the studied trilayer assemblies.

Layer	TA6V	Epoxy	Composite
ρ [kg/m^3]	4430	1300	1590
E [GPa]	113	5.12	10.5
ν	0.34	0.30	0.29
c_L [m/s]	6060	2300	2920
c_T [m/s]	3120	1230	1600
h [µm]	180	80 to 200	13600

ρ [kg/m^3]: density; E [GPa]: Young's modulus; ν: Poisson's ratio; c_L [m/s]: Longitudinal wave velocity; c_T [m/s]: Transversal wave velocity; h [µm]: layer thickness.

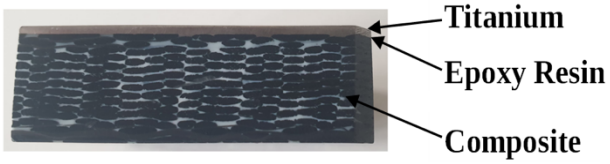

Figure 1. Cross-section view of the studied trilayer.

2.2 Scanning Acoustic Microscope (SAM)

The experimental study uses the PVA TEPLA Scanning Acoustic Microscope (SAM 301 - pulse-echo mode), which is based on the reflection of acoustic waves at interfaces due to changes in acoustic impedance. It is a sequential representation system in which a piezoelectric transducer emits a beam of ultrasonic waves which propagate through a coupling liquid, which is water in this case. The beam is scattered by the sample, and the signal is received by the same transducer [4, 5, 6]. As shown in Figure 2, the SAM consists of three main functional units: the acoustic sensor,

the electronic unit, the mechanical scanning system, and the display unit [7].

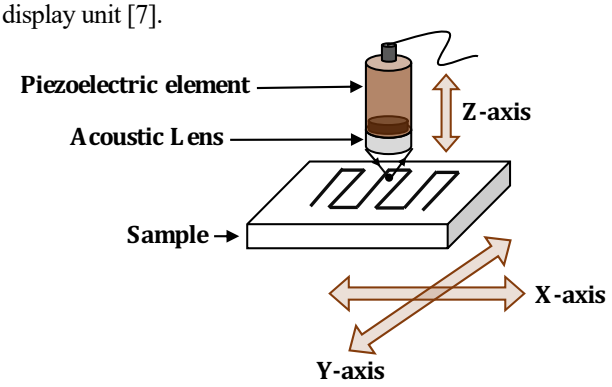

Figure 2. Scanning axes of the SAM.

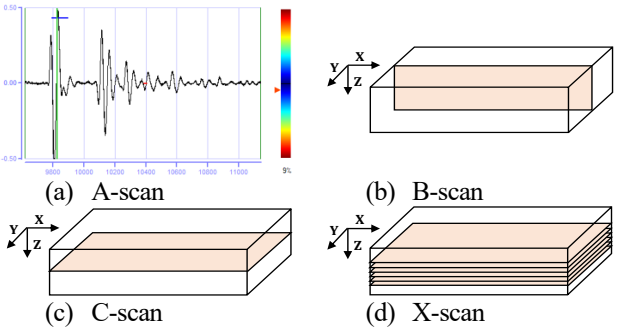

Figure 3. Types of scans for the visualization of ultrasound signals.

It also provides a variety of imaging options, as shown in Figure 3. Different types of scans are available, each offering a unique method of visualizing and assessing the material under examination. The four most commonly used scan types with SAM are A-scan, B-scan, C-scan, and X-scan [8].

3. CHARACTERISATION OF THE SAMPLES

Using the planar and focusing transducers available in the laboratory, background echoes from the adhesive were observed in samples with an Epoxy film thickness of less than 200 µm. This observation aligns with the fact that the adhesive is highly attenuating, and the energy of the echo at the Epoxy-Composite interface decreases with increasing Epoxy thickness. In this study, two samples with significant differences in the Epoxy film are examined: Sample 1 has a significantly thicker Epoxy film compared to Sample 2, as shown in Table 2.

3.1 Axial resolution consideration

The axial resolution (eq. 4) of the selected transducer must be adequate in relation to the thickness of the adhesive film being measured. This requirement is often expressed in terms of the thickness-to-wavelength ratio, which must be sufficient to allow effective echo separation. For a Gaussian echo envelope, the axial resolution is given by [9, 10]:

$$\Delta z_6 = \frac{t_6}{2T_0}\lambda_0 \approx \frac{0.88}{BW_{6,r}}\lambda_0 \qquad (4)$$

where Δz_6, t_6 and $BW_{6,r}$, represent respectively the axial resolution along the propagation axis, the round-trip signal duration, and the bandwidth at −6 dB, λ_0 and T_0 are the wavelength and the time period associated with the center frequency f_0. Consequently, the center frequency f_0 can be chosen so as to satisfy the following criterion:

$$f_0 \geq \frac{0.88}{BW_{6,r}} \max_{1\leq n\leq 3}\left\{\frac{c_{L,n}}{h_n}\right\} \qquad (5)$$

where $c_{L,n}$ is the longitudinal wave velocity and h_n is the thickness of the considered layer indexed n. In the studied case, with an estimated relative bandwidth of the transducer around $BW_{6,r} = 50\%$, the theoretical axial resolution limit at −6 dB is $\Delta z_6 = 1.76\ \lambda_0$. Thus, taking into account the thin adhesive layer into consideration, with a wave velocity of 2300 m/s in the Epoxy and a minimum thickness of 80 µm, eq. (5) gives a minimum center frequency f_0 of the transducer at 50 MHz.

A-scan characterizations are therefore performed using a planar transducer (Olympus V358-SU, SN: 1466080) with a center frequency of 50 MHz. As a result of eq. (4), the axial resolution of the system at 50 MHz is estimated at $\Delta z_6 \approx 81$ µm in the Epoxy layer. As an illustration, Figure 4 shows the A-scans obtained on samples 1 and 2.

3.2 A-scan

As a preliminary step, the caliper measurements of the thicknesses of the three constitutive layers are summarized in the following Table 2:

Table 2. Caliper measurements of thicknesses [µm].

Sample	TA6V	Epoxy	Composite
1	994	135	13540
2	981	86	13610

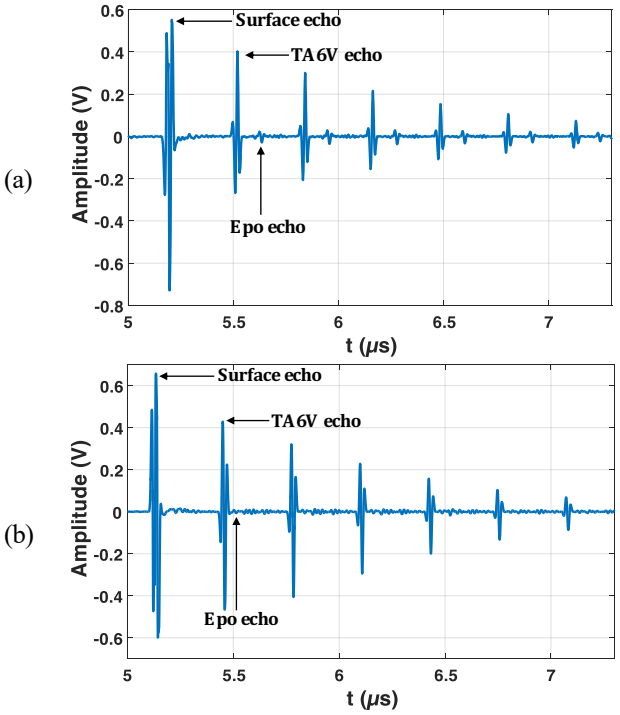

Figure 4. A-scan for 50 MHz center frequency excitation.: (a) Sample 1 and (b) Sample 2.

Upon examining the obtained signals in Fig.4, it can be observed: the echo reflected at the {Water/T} interface (first interface) labelled "Surface echo"; the echo reflected at the {Ti/Epo} film interface (second interface) labelled "TA6V echo"; a very small reflected echo at the {Epo/Comp} interface (third interface) labelled "Epo echo". Then are following periodically delayed multiple reflections from the TA6V layer, *i.e.* the {Ti/Epo} interface (second interface), as well as the associated small echoes from the {Epo/Comp} interface (third interface). The thickness of the adhesive film is then deduced by evaluating the time-of-flight between the background echo of TA6V (labelled "TA6V echo" on Fig.4) and the background echo of the Epoxy resin (labelled "Epo echo" on Fig.4), corresponding to the wave path within the Epoxy resin.

3.3 Determination of the Epoxy film thickness

This time-of-flight is estimated using the cross-correlation [11] between the Hilbert transform (HT) of the considered echoes indexed $n = \{1, 2\}$. The cross-correlation $cor_{e1,e2}(t)$ results from an integral between the envelopes $e_1(t)$ and $e_2(t)$ of the considered echoes $s_1(t)$ and $s_2(t)$, respectively:

$$cor_{e1,e2}(t) = \int_{-\infty}^{+\infty} e_1(\tau).e_2(t-\tau).d\tau \qquad (6)$$

with $$e_n(t) = \left|s_n(t) + i.HT\{s_n(t)\}\right| \qquad (7)$$

This envelope calculation (eq. 7) requires to pay a special attention of the studied echoes, as well as careful identification of the cutting boundaries of the echoes and a smooth windowing. The cross-correlation (eq. 6) shows a maximum at the date Δt_{max} which corresponds to the time-of-flight between the considered echoes $e_1(t)$ and $e_2(t)$.

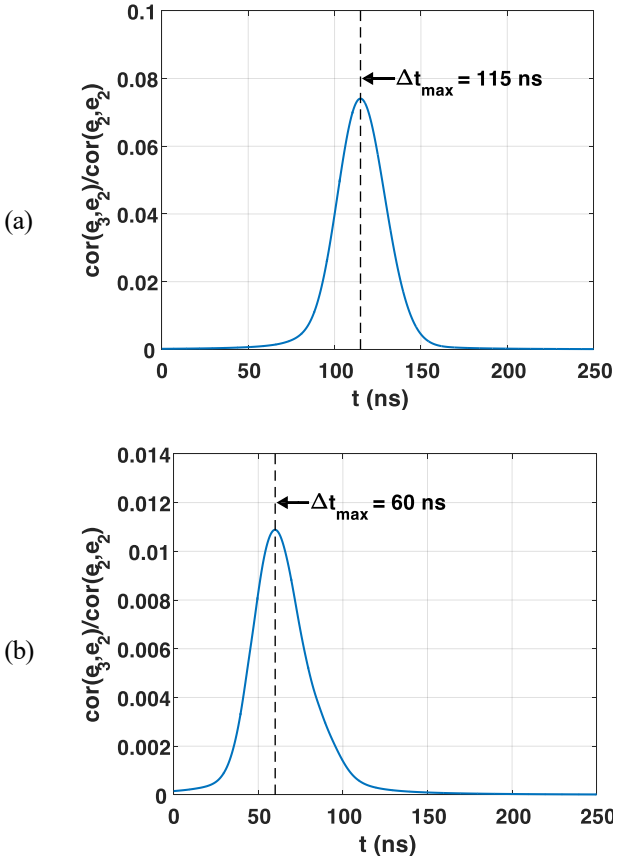

Figure 5. Cross-correlation of the Hilbert envelopes of the considered echoes of TA6V and Epoxy layers: (a) Sample 1 and (b) Sample 2.

As shown in Fig. 5, the calculated cross-correlation (eq. 6) of the Hilbert transform envelopes (eq. 7) of the relevant echoes, gives an evaluated cross-correlation time-of-flight Δt_{max} at 115 and 60 ns for samples 1 and 2, respectively. The thickness of the adhesive layer (Epoxy layer) is therefore estimated from the time-of-flight relationship: $e_{Epoxy} = c_L \times \Delta t_{max}/2$, giving in 132 µm and 69 µm for samples 1 and 2, respectively. These measurements are more accurate and more relevant than the subtraction estimation given in Table 2.

3.4 Hypothesis on the quality of the adhesion

Knowing that the samples were assembled with an Epoxy resin cured under the same conditions, it induces the same attenuation in the adhesive film. It can be seen that the background echo at the {Epo/Comp} interface is significantly higher for the thicker sample (sample 1, 132 µm), whereas the background echo at the {Ti/Epo} interface is almost the same for both samples. This amplitude difference between the two samples is assumed to be related to the quality of the adhesion at the {Epo/Comp} interface: a low level of adhesion in sample 1 leads to low transmission into the Composite and a high reflected echo, whereas a high level of adhesion in sample 2 results in higher transmission into the Composite and a lower reflected echo, as observed for this second sample. A series of C-scans, *i.e.* X-scans (Figure 3), are then performed to confirm this assumption.

3.5 X-scan

Using a 20 MHz focusing transducer, an X-scan is initiated to obtain 2D images (C-scans) reflecting the subsurface condition. Initially, it is essential to configure the experimental conditions, including setting the correct focal distance (with a fixed focus on the Epoxy background echo), calibration, and establishing the protocol for horizontal adjustment. The result will be C-scans at different depths within the sample. In addition, the focus was set on the Epoxy/Composite interface.

For all X-scan in this study, the gate size of each C-scan is 20 ns, corresponding to a distance of 23 µm in the Epoxy and 29.2 µm in the Composite. The axial resolution of the system at 20 MHz is 202 µm in the Epoxy.

A data window was selected and then divided into C-scan windows of 20 ns each. The scan area is 2 cm × 1.5 cm^2 with a pixel resolution of 200 µm/Pixel for sample 1 and 2×2 cm^2, with a pixel resolution of 100 µm/Pixel for Sample 2.

Analysing the images resulting from the X-scan starting from the TA6V-Epoxy interface (Figure 6a) for Sample 1, uniform colours are observed over most of the image, with some contrast at the edges, possibly indicating a slight misalignment of the sample. This colour homogeneity suggests that the medium remains unchanged, meaning we are still within the Epoxy layer. As we progress through the images, we reach C-scan n°7 where we can confirm the transition from the Epoxy to the Composite layer by the presence of carbon fibre bundles. By measuring the time shift between C-scan n°1 and C-scan n°7, corresponding to six windows of 20 ns each, the thickness of the Epoxy layer can be estimated as follows: $e_{epoxy} = 6 \times 23 = 138$ µm.

For Sample 2 (Figure 6b), a similar pattern is observed. The image shows a uniform color distribution, indicating that we are still within the Epoxy layer. As we analyze the successive images, C-scan n°4 shows the presence of carbon fibre bundles in light blue, mixed with the Epoxy in dark blue. This marks the transition from the Epoxy layer to the Composite zone, as the fiber bundles become clearly visible across several image windows. The thickness of the Epoxy layer is then estimated from the time shift between C-scan n°1 and C-scan n°4, corresponding to three windows of 20 ns each: $e_{Epoxy} = 3 \times 23 = 69$ µm.

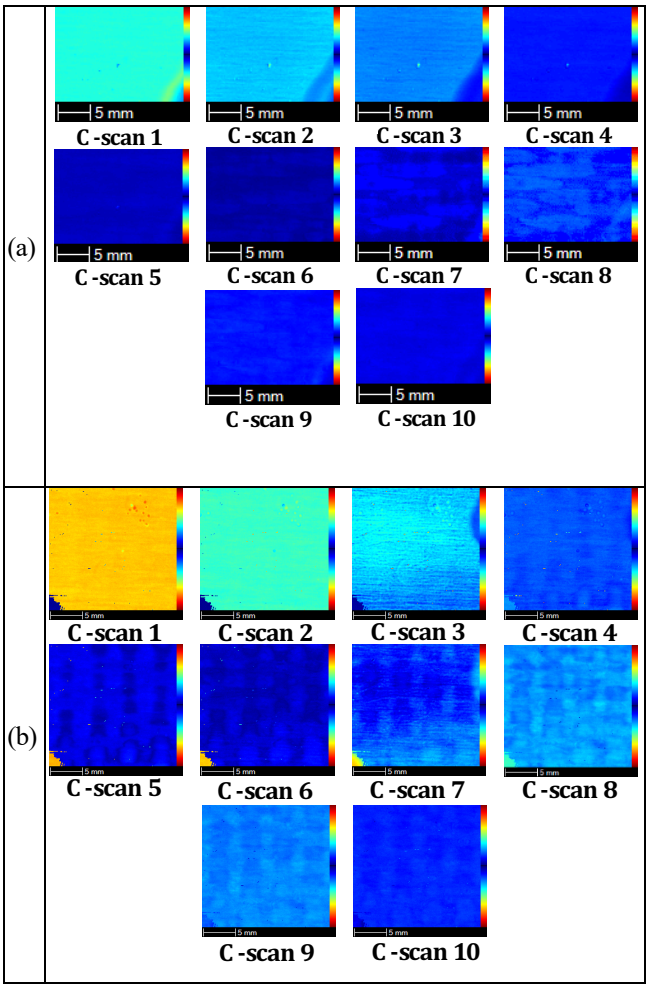

Figure 6. X-scan starting from the TA6V/Epoxy interface: (a) Sample 1 and (b) Sample 2.

Table 3 summarizes the measured thickness of the adhesive film by the three methods: the basic measure by the calipper, by X-Scan and A-Scan.

Table 3. Epoxy film thickness [µm] according to measurement method.

Method	Sample 1	Sample 2
Calliper	135	86
X-scan	138	69
A-scan	132	69

The A-scan measurement estimates it to be 132 µm, while the X-scan imaging gives a thickness of 138 µm. For sample 2, both methods give a thickness of 69 µm for the Epoxy layer. The A-scan method is the most accurate, but the X-scan can provide a quick estimate of the thickness of the Epoxy, although it is highly dependent on the time gate size and its initial starting position.

As shown in Figure 6, in terms of bond quality, the Composite is detected in several X-scan imaging windows of the same duration (20 ns): in sample 2 (spanning six C-scan windows, from C-scan n°4 to n°9). In contrast, it appears in only two X-scan imaging windows for sample 1 (C-scans n°7 and n°8) and is less distinct. These observations show how the transmitted echoes propagate through the Composite and allow the carbon fibers to be distinguished from the Epoxy. The number of detected C-scan images, which reflects the depth of the signal penetration into the Composite, confirms that the adhesion is stronger in Sample 2 than in Sample 1.

4. DISCUSSION

Initially, several samples with different adhesive film thicknesses were tested using either planar or focused transducers. Pulse-echo measurements showed that only samples with an adhesive film thickness of less than 200 µm exhibited round-trip echoes. This finding is consistent with the fact that the adhesive is highly attenuating, causing a further reduction in the energy reaching the {Epo/Comp} interface as its thickness increases. Two samples made of the studied trilayer structure {Ti/Epo/Comp} have been studied (see Table 2).

Accurate precise measurement of the Epoxy film thickness is essential to ensure the mechanical properties of the adhesive. In practice, strips of material placed on the edges of the surfaces between the two materials during the bonding process allow the thickness to be controlled. However, this thickness can change during polymerization. Therefore, the thickness measurement after the bonding operation is only an estimate that must be validated by acoustic methods. The measurement of the Epoxy film thickness for Sample 1 was 132 µm with the A-scan compared to 138 µm with the X-scan. However, for Sample 2, the thickness is 69 µm with A-scan and 69 µm with X-scan, compared to an estimate of 86 µm, indicating that the estimate is inaccurate and that the thickness to be taken into account is that obtained by acoustic method.

In terms of adhesion quality and comparing the results of the two samples, it can be seen that for Sample 2, with an Epoxy film thickness of 69 µm, the background echo amplitude is low. Conversely, for Sample 1, with an Epoxy film thickness of 132 µm, approximately double of that of Sample 2, the background echo amplitude is significant. This difference in amplitude cannot be attributed to the attenuation due to the viscosity of the adhesive but rather to interface conditions. This leads to the hypothesis that the adhesion quality of sample 2 is better than that of sample 1, the cohesive properties of the adhesive being identical.

In X-scan imaging, the Composite fibers are visible in several C-scan windows of the same duration (20 ns). For sample 2, the Composite fibers can be observed in 6 consecutive C-scan windows, whereas for sample 1, they are less visible, appearing in only 2 C-scan windows. This can be interpreted as a better energy transmission from the adhesive film to the Composite, suggesting a degraded adhesion quality in sample 1 compared to sample 2. These observations highlight the energy transmission within the Composite and allow the differentiation of the carbon fibers, with different levels of clarity in the different windows. As a result, the X-scan imaging supports the hypotheses derived from the A-scan analysis regarding adhesion quality.

Thus, regarding the background echo amplitude of the Epoxy film which depends on the {Epo/Comp} interface and the related adhesion quality, it can be concluded that the adhesion quality of Sample 2 is better than that of Sample 1.

5. CONCLUSION

The challenge of the ultrasound investigation lies in the very contrasting impedance discontinuities in the studied trilayer {Ti/Epo/Comp} structure: strong between the titanium and the adhesive, and weak between the adhesive and the Composite. These samples were characterized using the scanning acoustic microscope PVA TEPLA SAM 301. One of the objectives was to evaluate the thickness of the Epoxy film. Quantification using X-scan imaging was also carried out to obtain different C-scans in depth, particularly

from the Epoxy to the Composite, allowing the thickness of the epoxy film to be measured by imaging. The different levels of adhesion in the samples were identified by analyzing the background echo of the Epoxy film relative to its thickness, and by examining the amount of energy transmitted to the Composite layer through the X-scan imaging.

6. ACKNOWLEDGMENTS

The authors would like to thank the Le Havre Seine Metropole (LHSM) and the Normandy region for supporting the funding of this PhD work.

7. REFERENCES

[1] R. Hodé, S. Raetz, J. Blondeau, N. Chigarev, N. Cuvillier, V. Tournat and M. Ducousso, "Nondestructive evaluation of structural adhesive bonding using the attenuation of zero-group-velocity Lamb modes", Applied Physics Letters, vol. 116, p. 104101, 2020 (https://doi.org/10.1063/1.5143215).

[2] M. Ducousso, S. Bardy, Y. Rouchausse, T. Bergara, F. Jenson, L. Berthe, L. Videau and N. Cuvillier, "Quantitative evaluation of the mechanical strength of titanium/composite bonding using laser-generated shock waves", Applied Physics Letters, vol. 112, p. 111904, 2018 (https://doi.org/10.1063/1.5020352).

[3] L. Attar, M. Ech Cherif El Kettani, D. Leduc, M. V. Predoi and J. Galy, "Detection of kissing bond type defects and evaluation of the bonding quality in metal/adhesive/composite structures by a wavenumber-frequency insensitive SH mode", NDT & E International, vol. 137, p. 102841, 2023 (https://doi.org/10.1016/j.ndteint.2023.102841).

[4] R. A. Lemons and C. F. Quate, "Acoustic microscope - Scanning version", Applied Physics Letters, vol. 24, p. 163–165, 1974 (https://doi.org/10.1063/1.1655136).

[5] R. A. Lemons and C. F. Quate, "Integrated circuits as viewed with an acoustic microscope", Applied Physics Letters, vol. 25, p. 251–253, 1974 (https://doi.org/10.1063/1.1655459).

[6] V. Jipson and C. F. Quate, "Acoustic microscopy at optical wavelengths", Applied Physics Letters, vol. 32, p. 789–791, 1978 (https://doi.org/10.1063/1.89931).

[7] F. Hamdi, S. Bouhedja and H. Amrani, "Theoretical study of different attenuation measurement by acoustic microscopy", Journal of Applied Physics, vol. 114, p. 133501, 2013 (https://doi.org/10.1063/1.4823850).

[8] F. Bertocci, A. Grandoni and T. Djuric-Rissner, "Scanning Acoustic Microscopy (SAM): A robust method for defect detection during the manufacturing process of ultrasound probes for medical imaging", Sensors, vol. 19, p. 4868, 2019 (https://doi.org/10.3390/s19224868).

[9] N. Samet, P. Maréchal and H. Duflo, "Ultrasonic characterization of a fluid layer using a broadband transducer", Ultrasonics, vol. 52, pp. 427-434, 2012 (https://doi.org/10.1016/j.ultras.2011.10.004).

[10] N. Samet, P. Marechal and H. Duflo, "Ultrasonic imaging of bubble motion in a fiber preform", in Proceedings of the Acoustics 2012 Conference, pp. 2601-2606, 2012 (https://hal.science/hal-00810855).

[11] N. Ghodhbani, P. Marechal and H. Duflo, "Ultrasonic broadband characterization of a viscous liquid", Ultrasonics, vol. 56, pp. 308-317, 2015 (https://doi.org/10.1016/j.ultras.2014.08.013).